UCRL-11334

University of California

Ernest O. Lawrence Radiation Laboratory

TWO-WEEK LOAN COPY

This is a Library Circulating Copy which may be borrowed for two weeks. For a personal retention copy, call Tech. Info. Division, Ext. 5545

THE ENERGY CONVERSION CHARACTERISTICS OF A BRUSHLESS DIRECT CURRENT SERVOMOTOR

Berkeley, California

DISCLAIMER

This document was prepared as an account of work sponsored by the United States Government. While this document is believed to contain correct information, neither the United States Government nor any agency thereof, nor the Regents of the University of California, nor any of their employees, makes any warranty, express or implied, or assumes any legal responsibility for the accuracy, completeness, or usefulness of any information, apparatus, product, or process disclosed, or represents that its use would not infringe privately owned rights. Reference herein to any specific commercial product, process, or service by its trade name, trademark, manufacturer, or otherwise, does not necessarily constitute or imply its endorsement, recommendation, or favoring by the United States Government or any agency thereof, or the Regents of the University of California. The views and opinions of authors expressed herein do not necessarily state or reflect those of the United States Government or any agency thereof or the Regents of the University of California.

Research and Development

UCRL-11334

UNIVERSITY OF CALIFORNIA

Lawrence Radiation Laboratory
Berkeley, California

AEC Contract No. W-7405-eng-48

THE ENERGY CONVERSION CHARACTERISTICS OF A BRUSHLESS DIRECT CURRENT SERVOMOTOR

Donald Raymond Machen

(M. S. Thesis)

March 16, 1964

Printed in USA. Price $1.25. Available from the
Office of Technical Services
U. S. Department of Commerce
Washington 25, D.C.

THE ENERGY CONVERSION CHARACTERISTICS OF A BRUSHLESS DIRECT CURRENT SERVOMOTOR

Contents

Abstract v

I. Introduction 1

A. History 1

B. A New Need for Brushless dc Machinery 4

C. The Development of the Solid-State Switch 5

D. Other Experimental Brushless Motors 9

II. The Permanent Magnet Machine 12

A. Design of the Two-Phase Converter 15

B. The Phase-Locking Networks 21

C. Specifications on Converter Design 23

III. Experimental Results and Conclusions 27

A. Instrumentation Methods 27

B. Discussion of Torque-Speed Curves 30

C. Recommendations for Future Work 33

D. Conclusions 35

Acknowledgments 37

Appendix. Development of the Torque Equation for a Two-Phase Synchronous Machine with a Permanent Magnet Rotor

A. Derivation of the Torque Equation 38

B. Reference Frames 38

C. Electric-Force Formulation from Energy Consideration 40

D. Magnetic Vector Potentials 41

E. Formulation of the Air-Gap Energy 43

List of Symbols 48

Bibliography 50

THE ENERGY CONVERSION CHARACTERISTICS OF A BRUSHLESS DIRECT CURRENT SERVOMOTOR

Donald Raymond Machen

Lawrence Radiation Laboratory
University of California
Berkeley, California

March 16, 1964

ABSTRACT

The energy conversion characteristics of a direct-current servomotor without commutating brushes are investigated in this thesis.

The development of the excitation system and the final characteristic parameters of the brushless machine are considered. The analytic treatment of the energy-conversion mechanism within the machine is carried out by the application of Maxwell's equations in the air gap. An expression for the electrically developed torque is derived (by energy methods), which is applicable to the brushless machine within the limits of the assumptions made.

I. INTRODUCTION

The direct-current motor, which serves either as a prime mover or as a control-system servomotor, provides a most desirable torque-speed characteristic along with ease of rotational velocity control not necessarily enjoyed by other classes of electromechanical energy converters.

A prime disadvantage of the direct-current machine is the need for commutating brushes between the stationary and moving members. Brushes produce a very real maintenance problem to normal users of machinery and cannot be used in a high-altitude or space application without the machine's being completely sealed in a pressurized container. Brushes have also proved to be hazardous in an explosive atmosphere.

For the above reasons, the direct-current motor would be a more generally useful device than it already is, provided the commutating brushes could be removed.

A. History

The possibility of removing the brushes is not by any means new. Several investigators, prior to World War II, reported on methods of operating machine systems on direct current without brushes. The commutator, at least during those years, was not a truly perfected component of an electric machine and was, as it is now, a source of inefficiency.

The first published attempt to utilize the thyratron as a switch for replacement of the commutator segments in a dc machine should be attributed to Alexanderson in 1934.[1] His system was complete and marketable; however, there were some major disadvantages: (a) The scheme, compared with bar commutators, was very costly; (b) space requirements were excessive; and (c) the circuitry required for adequate commutation was complex.

In spite of the disadvantages, it is interesting to consider the basic mechanism of the Alexanderson motor as quoted from the original paper:

"Through the commutator function, a motor is made available which operates on an a-c line but has the smooth variable speed-torque characteristics like a d-c motor without any reference to synchronism to the a-c system."

The basic system proposed by Alexanderson utilized thyratrons not only to switch current in stationary armature coils but to rectify ac line current as well. Control of the thyratrons was accomplished by using an auxiliary distributor mechanically coupled to the motor shaft. The machine was similar to a synchronous motor because the rotor maintained a constant field within the machine. Motor starting and low-speed commutation were achieved when the ac line voltage passed through zero. At medium and high speeds the grid control and back emf of the winding served to provide commutation.

Also in 1934, Willis published a paper describing his scheme for a brushless dc motor.[27] The Willis motor was similar to that of Alexanderson, as the motor consisted of a stationary armature and rotating field, but the armature windings were switched by single thyratrons -- one per winding. The main source of power was dc rather than ac, and low-speed commutation was achieved by use of a cathode resistance-capacitance network, as shown in Fig. I-1. At high speeds, the thyratrons turned off because of the back emf of their windings when another winding was switched on.

It can be assumed -- although it is not so stated in the journals -- that the war effort brought to a halt any further plans in the development of brushless machinery. Efforts to perfect the bar commutator continued, as it was badly needed for many wartime applications.

Others have attempted to modify the dc motor (or generator). Kuebler derived dc motor speed characteristics from a three-phase synchronous machine.[15] He incorporated 3-phase rectifiers that fed thyratrons, which, in turn, were switched by a control voltage from an auxiliary (low current) commutator and applied power to the armature windings. His system produced series motor characteristics; however, the system does not seem to be much of an improvement over the Alexanderson or Willis machines.

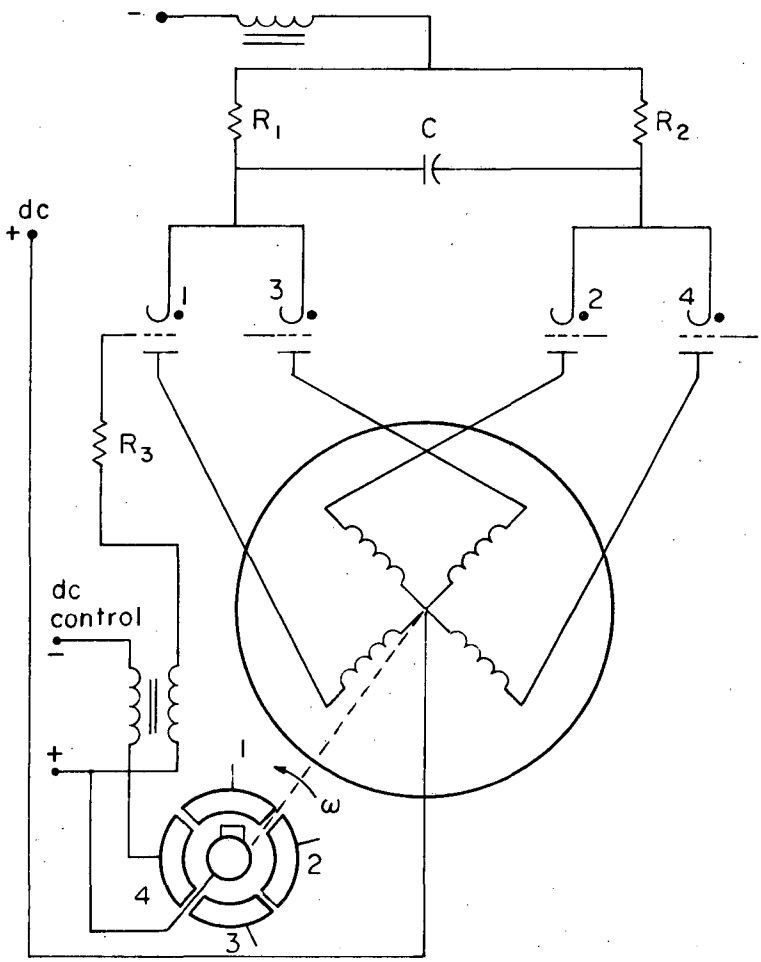

MU-33980

Fig. I-1. Diagram of Willis motor.

Ishizaki[14] and Steiger[22] have studied the effects of rectified ac from thyratrons for use in driving dc-series servomotors. They did not, however, attempt to remove the brushes from the dc machines. The main point of their work was to study the heating effects of rectified ac (compared with pure dc) on the machines.

B. A New Need for Brushless dc Machinery

As direct-current power equipment became an integral component for aircraft, people began to investigate the possibilities of inserting high-efficiency silicon rectifiers within the rotor and shaft structure of dc exciter generators. An ac synchronous generator rotor could then be mounted on the same shaft, with the field connections brought through the shaft to the dc provided by the small excitor generator. Ford showed the advantages of this type of system and discussed the workable 40- and 50-kVA compact generating systems now operational on some British aircraft.[13]

The problem of operating dc machinery at high altitude and low pressure is becoming more acute as man strives toward space travel, where the normal environment is a continual and complete vacuum. Control systems requiring servomotors for positioning or general transformation of analog signals to motion are required throughout such spacecraft. Power generation in space, at least for the presently foreseeable future, could be limited to high-power-density direct current. The formation of alternating current for general power requirements would be a costly and complex undertaking. Examples of the type of space power now operational or under development are (a) normal battery power with solar-cell recharging, (b) nuclear thermionic diodes, and (c) magnetohydrodynamic channels. These three systems provide the spacecraft with direct current of very high power density -- ideal as power sources for servosystems using dc servomotors as control components. However, the fact remains that dc servomotors with brushes do not function reliably in a vacuum.

C. The Development of the Solid-State Switch

In the mid-1950's Royer published a paper dealing with the development of a power converter with switching transistors.[19] The basic unit, shown in Fig. I-2a, consists of two power transistors and a saturable-core transformer of high permeability. The transistors are operated in a manner such that the transformer output is square-wave ac, of a frequency proportional to the magnitude of the dc applied to the converter.

Royer's dc to ac converter opened the way for the 1950 series of experimental brushless dc motors. The idea was to provide a small, high-power converter to serve as a source for the motor. The motor could be of the same basic type as the Alexanderson motor or, perhaps, a two-phase induction servomotor used in many control systems. The overall system looks like a dc machine, and speed control is accomplished by control of the input dc voltage to the converter.

In 1955, Brailsford published a series of papers dealing with the commutatorless dc motor.[3, 4, 5] Figure I-3 depicts his basic circuit. The Brailsford motor may be compared to a single-phase synchronous motor that "makes its own ac" of the appropriate frequency at any speed. Although similar to the single-phase synchronous motor, this motor does not start by itself, runs equally well in both directions, and relies on the inertia of the rotor to "average out" the pulsating torque. Brailsford and Company manufactures several brushless dc motors for use as small low torque producing machines, such as a fan motor, etc. The torque-speed characteristics of the Brailsford motor are essentially those of the series dc motor.

In 1955, Milnes,[17] and in 1959, Card[9] showed that switching transistor dc to ac converters can be operated in a phase-locked mode at any desired phase angle.[17, 9] The 90° phase-locked converters are of interest, if one considers using a two-phase machine to achieve brushless operation. Card's converter is shown in Fig. I-4.

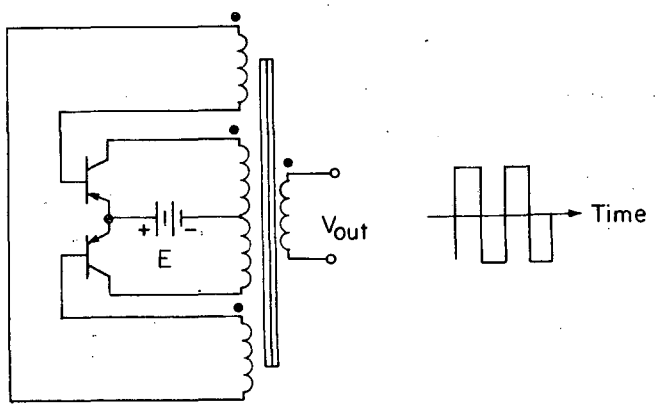

(a)

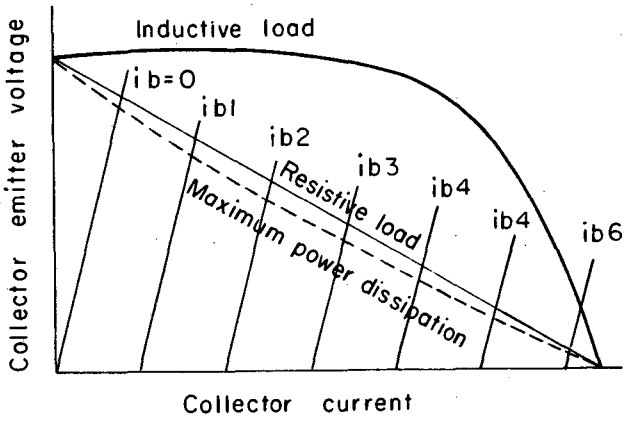

(b)

MU-33981

Fig. I-2. Typical transistor dc to ac converter and PNP transistor switching-characteristics common emitter.

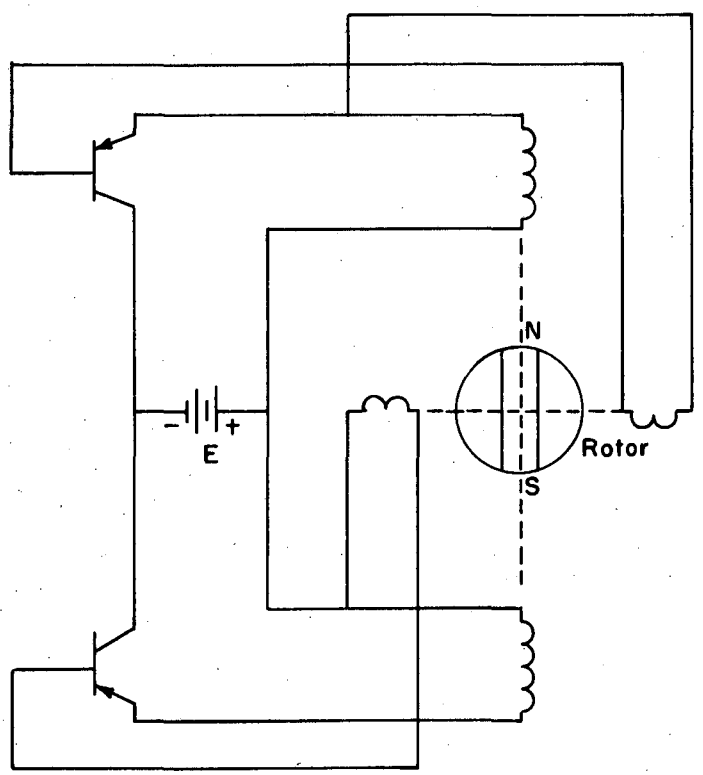

MU-33982

Fig. I-3. The Brailsford motor.

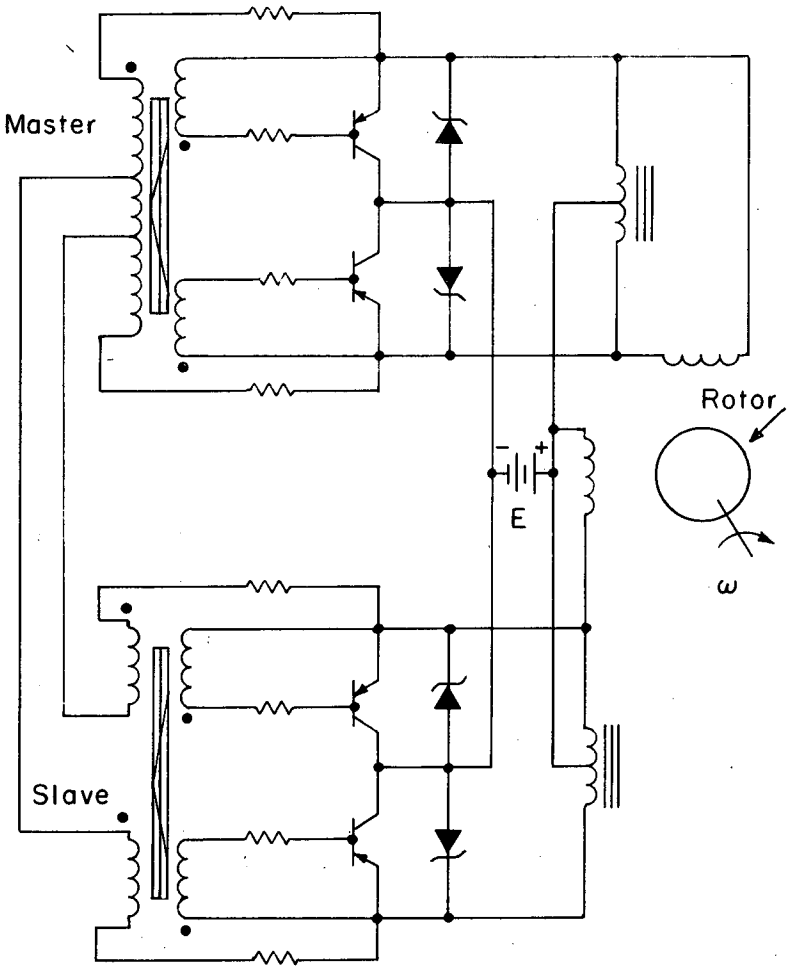

MU-33983

Fig. I-4. Card's phase-locked dc to ac converter.

It should be noted here that a major problem in operating a transistor switching circuit into an inductive load is the high collector-emitter voltage transients that may occur during operation. Figure I-2b depicts a typical transistor characteristic curve (collector-emitter voltage vs collector current) with base current as a parameter. Load lines for switching mode operation are shown for both resistive and inductive loads. The transient increase in V_{CE} (voltage-collector to emitter) can be seen for an inductive load. Both curves are above the maximum power dissipation curve; however, the switching operation occurs at a speed that causes the average power dissipated to be within the ratings of the transistor. These switching transients may be reduced to a level such that they do not exceed the maximum allowable V_{CE} of the transistor, by deliberately slowing the switching action at the expense of increased power dissipation. Reverse voltage is reduced by a Zener diode network across the collector-emitter terminals.

The use of transistors in the switching mode and saturable core transformers to provide the ac necessary to excite small ac servomotors (or large prime movers) is indeed an approach to the brushless dc machine. Other methods of accomplishing the above have been published since the late 1950's, however.

D. Other Experimental Brushless Motors

Other recent work in the field of brushless motors has been done by Schwartz[21] and Eisenlohr[11] of Massachusetts Institute of Technology, and by Trickey[23] of Wright Machinery Company. Both the MIT and the Trickey systems utilize switching transistors or silicon controlled rectifiers with some form of auxiliary commutator in order to sense rotor position for proper firing of their solid-state devices. The auxiliary rotor-position sensing devices were Hall transducers, and small saturable reactors provided a usable signal for actuating triggers, bistable flip-flops, and other switching networks comprising the motor exciter.

The MIT and Trickey systems do produce the desired series motor characteristics; however, the fact that they still incorporate some form of commutation -- even though it is not of the bar and brush type -- reduces the utility of the system as a whole.

In 1962 a series of articles was published containing questions to and replies from well-known machinery and systems engineering firms concerning brushless dc motors.[16] This recent interest among manufacturers indicates that perhaps renewed enthusiasm in the brushless motor is here to stay, but one can only conjecture on this point.

During the past year several other motor manufacturers have advertised brushless dc motors as a regular product line. The Lamb Electric Company markets a dc machine that uses two transistor switches operating into the stator windings of the motor and uses the stator steel as the switching core. The motor is, in reality, a wound rotor induction motor, but the overall system is a dc motor without brushes. They state that their machines are available from 1/50 to 2 horsepower ratings. Globe Industries also markets several variations of a brushless dc motor, as does the Barber-Colman Company (type YAD). This motor is designed for fan loads with a 12-V dc input, no-load speed of 4600 rpm, and a starting torque of 0.053 lb. in. The motor torque-speed curve is shown in Fig. I-5.

It has been said that during the discussion of Trickey's recent paper at the 1962 American Instutute of Electrical Engineers (AIEE) Fall General Meeting in Chicago, a representative of a leading dc motor manufacturer asked, "Why try to remove the commutator now that we have it optimized as never before?" This question is a good one; however, as was mentioned earlier, brush and bar commutators do not function in high altitude or in space vehicles. The present and future power sources for spacecraft will probably be direct current; therefore, servomotors and other machinery might just as well be operated by direct current. This is at least one justification for continued interest in brushless machinery.

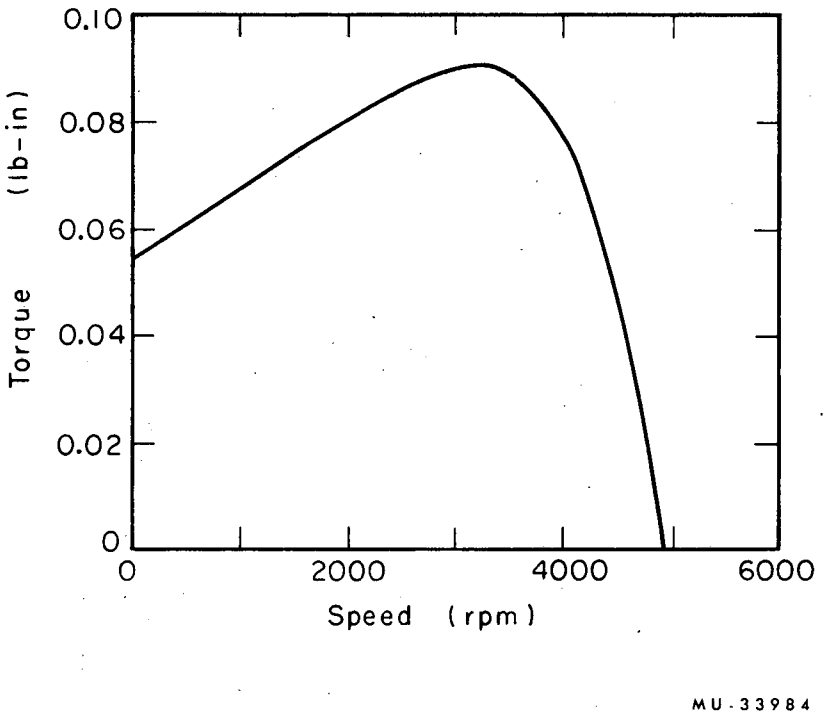

Fig. I-5. Torque-speed characteristics for Barber-Colman 12-V brushless dc motor.

II. THE PERMANENT MAGNET MACHINE

Many schemes for achieving brushless operation of dc machines have been proposed in the past. There are several available on the engineering market at present. These machines do in fact operate from dc sources; however, the torque-speed characteristics sometimes leave much to be desired.

The system proposed in this thesis not only accomplishes the removal of the commutating brushes but provides a constant torque with varying speed for any level of shaft loading.

The experimental device chosen for this research was a two-phase stator, permanent-magnet rotor, tachometer generator. The proposed system is shown in block diagram form in Fig. II-1. The machine, when excited by two-phase sinusoidal current, ran as a motor with excellent results up to 4000 rpm. In order to provide an overall brushless dc servomotor package, the exciter selected for the system was a two-phase switching transistor (dc to ac) converter.[17] The idealized output of the converter is shown in the lower section of Fig. II-1.

A major advantage of the proposed system is the complete lack of any type of commutating device, however small. Many of the machines proposed in the past contain small low-current commutators in order to control high-current switching devices, which in turn discharge into the machine windings.

The speed of the synchronous brushless dc machine is directly proportional to the magnitude of the applied input voltage to the converter. Therefore speed control is accomplished with ease.

The torque available to any external system coupled to the motor shaft is given (see Appendix) by

$$T_e = K I^s \sin\delta, \qquad \text{(II-1)}$$

where K is a constant determined by the machine parameters only, I^s is the peak value of the phase current, and δ is the torque angle, as used in normal synchronous machine theory.

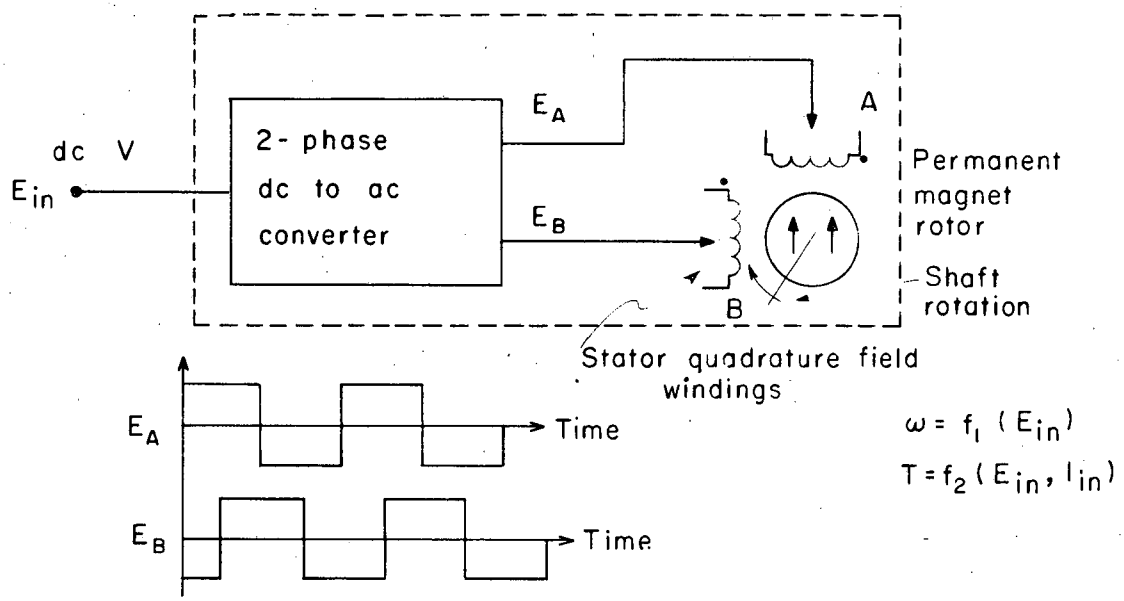

MU-33985

Fig. II-1. A scheme for brushless dc operation of a servomotor.

Inspection of Eq. (II-1) reveals that the torque is not in any way a function of the excitation frequency or motor speed. For any speed determined by the magnitude of the input dc voltage, the developed torque is determined by the phase current, a machine constant, and the sine of the torque angle. The angle δ varies from 0 to π radians, depending on the applied load and other factors; also I^s adjusts itself in such a way that the developed torque exactly equals the external torque applied by the load.

The theoretical torque vs speed curves are thus a family of curves, each having zero slope as shown below.

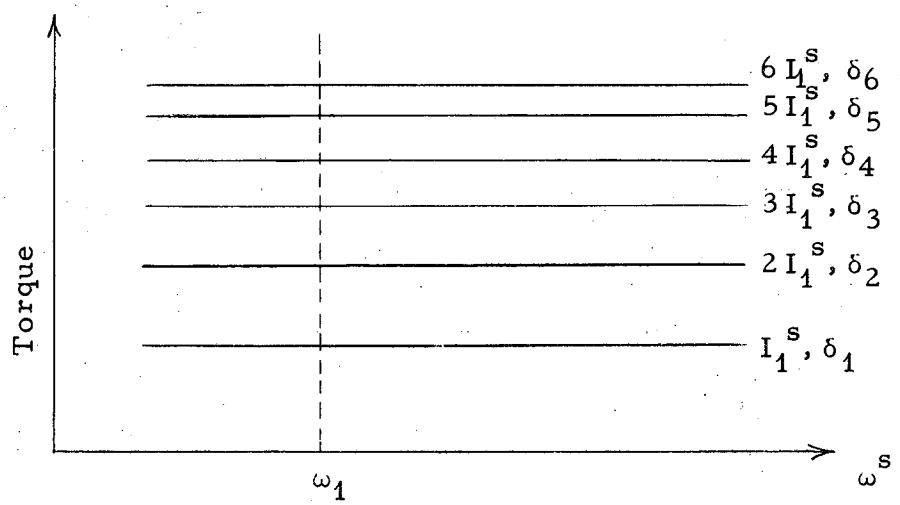

For any speed ω_1, the torque varies as the sine of the angle δ as the external load is increased. At some critical value of torque angle the stability limit is reached, and pullout (loss of synchronism) occurs. Operation beyond the pullout point is not considered in this thesis, as this is regarded as unstable operation.

The specific nameplate information for the experimental motor and information pertaining to its construction are listed below.

Experimental Motor Nameplate Information

General Electric Company

Type CM-5

Model 2CM5 - BAN

Serial 2757092

Two pole

Rotor type -- permanent magnet

Rotor OD -- 1.5 in.

Rotor length -- 1.0 in.

Stator ID -- 1.532 in.

Air gap -- 0.0313 in.

Number stator slots -- 12

Two phase windings of equal turns

Resistance per phase at 25°C -- 1400 Ω

Maximum rms phase current for 50°C temperature rise -- 100 mA.

Figure II-2 is a photograph of the experimental motor, showing the internal construction.

It should be noted at this point that the starting torque available from the experimental motor varied as an inverse function of the excitation frequency. None of the normal mechanisms for providing starting torque were incorporated in the machine. This fact did not affect the general outcome of the project, as torque-speed curves were obtained by means of a reaction torque dynamometer. (Instrumentation is covered in Chapter III.) A paper has been written proposing a method of incorporating starting torque features into permanent magnet rotor machines.[7] It is felt that any further work on the synchronous brushless dc motor should deal with the starting torque problem.

A. Design of the Two-Phase Converter

The form of the converter selected for use in this project was first proposed by Milnes in 1955.[17] The unit is basically two Royer dc to ac converters coupled together at the output, and with feedback

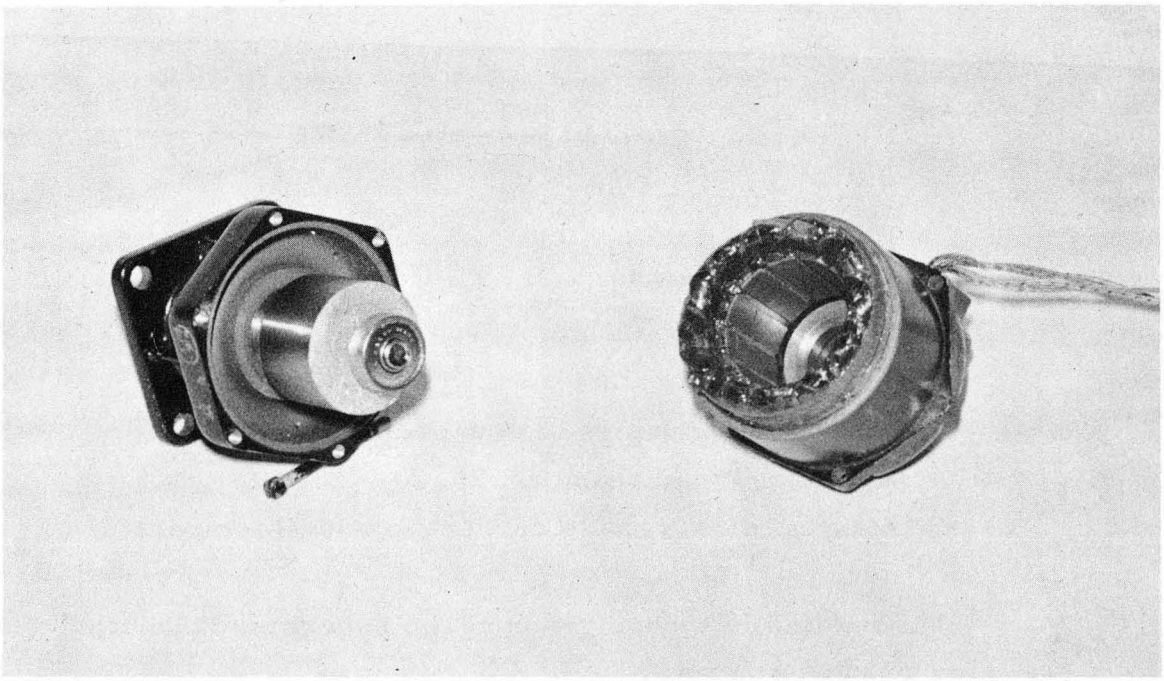

ZN-4259

Fig. II-2. The experimental motor.

to the switching transistors such that the output of one converter lags the other by 90 electrical degrees.[19]

The requirements of the experimental motor were specified, and circuit parameters were selected for the converter. Figure II-3 shows the circuit schematic and selected component values for the converter used in this thesis project. A brief outline of the theory of operation and design methods is included below.

The operating characteristics of the converter are determined by the properties of the saturable core material used to form the toroidal transformers. The number of turns making up the main switched windings and the core area also play an important part.

The cores selected were 2-mil-thick tape wound toroids of high-quality "square loop" magnetic steel called Orthonol (trade name). High efficiency is gained by using the toroidal form and by using the low-loss material mentioned. The core steel is fully utilized in that the flux is driven to positive and negative saturation on alternate half cycles of operation. This, in turn, induces alternating square wave voltages in the windings.

The basic equations describing the operation of a single converter may be stated, as follows:

Under ideal conditions, the voltage across the main switched winding at any instant in time is

$$e = nA \frac{dB}{dt} \quad , \qquad \text{(II-2)}$$

where n is the number of turns,

A is the core area (meters^2),

B is the flux density (webers/meters^2),

and e is the "core" voltage.

Now, assume that the core is initially at negative saturation. The application of a positive voltage of average value E drives the core flux to positive saturation in some time τ (assuming the proper magnetizing current is allowed to flow). At this point in time the voltage is automatically reversed, and the core flux is driven back

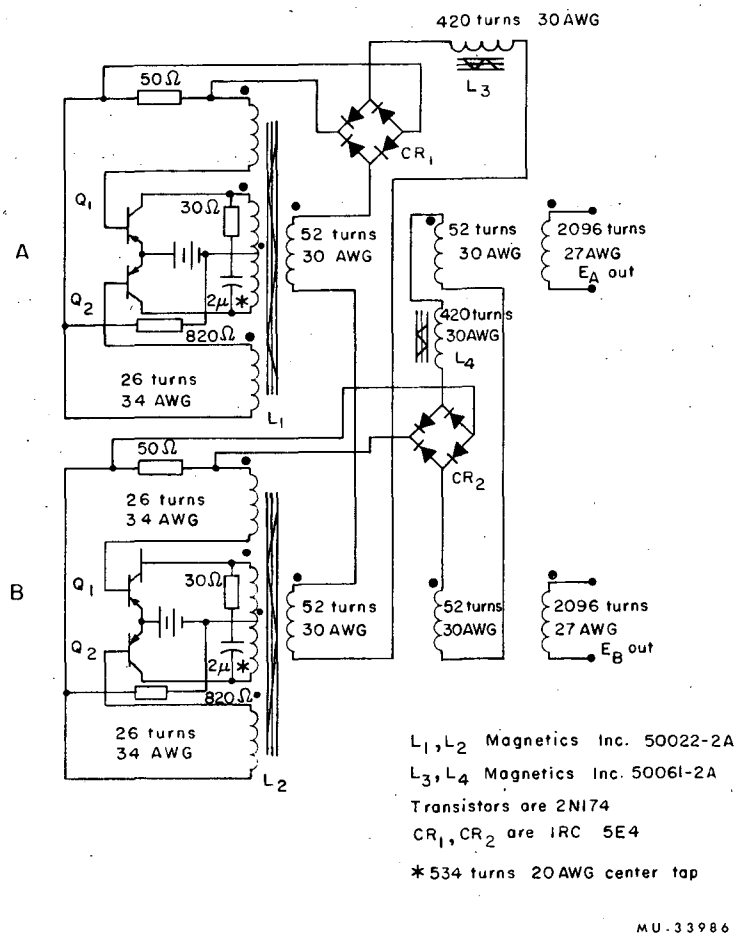

Fig. II-3. Two-phase transistor converter.

to negative saturation again. Repetition of the above action causes alternating square wave voltages to be induced in any other windings around the core. The magnitude of these voltages is dependent upon the turns ratio from the main winding to the winding in question.

Equation (II-2) may be written as

$$\int_0^{\tau} E\,dt = nA \int_{-B_s}^{+B_s} dB, \qquad \text{(II-3)}$$

where τ is the half-cycle period of output, B_s is the saturation flux density, and E is the average applied voltage to winding, or

$$\tau = \frac{2nA}{E} B_s. \qquad \text{(II-4)}$$

The half-cycle period τ may be rewritten as $1/2f$, where f is the oscillation frequency or output frequency of the converter.

Therefore,

$$f = \frac{E}{4nAB_s} . \qquad \text{(II-5)}$$

The product, $E\tau = 2nAB_s$, is the well-known volt-time rating of a core.

It is evident from Eq. (II-5) that the output frequency is directly proportional to the applied average voltage E. (Also E may be the dc voltage supplied to the converter.)

The two transistors incorporated in each converter in Fig. II-3 serve to switch or reverse the applied voltage (dc) when the core has reached saturation. Consider transistor Q_1 in the upper circuit of Fig. II-3 as being on or able to conduct from emitter (arrow) to collector at the instant we wish the unit to be energized. A current flows through Q_1 into the dotted upper section of the main winding, and the dc voltage of the driving source (less any emitter-collector drop in Q_1) appears across this section of the main winding. The core flux is driven positive and toward positive saturation.

Now, the transistors used are P-N-P power transistors. A negative voltage is required between base and emitter to cause the emitter-collector path to conduct. As the core flux is going positive, a negative voltage is induced on the base of Q_1 from the feedback winding associated with it that tends to turn Q_1 on border. At the same time a positive voltage is being induced on the base of Q_2 by the feedback winding associated with it. This voltage keeps Q_2 off.

When the core reaches positive saturation, the rate of change of flux density goes from positive to zero in a very short period of time. This negative dB/dt, occurring at the instant saturation is reached, induces voltage spikes into the feedback windings mentioned above. The polarity of these spikes is opposite to the polarity of voltages induced during the previous passage of time as the core flux was positive. Transistor Q_1 is forced off (or its conduction reduced greatly), and transistor Q_2 is turned on to the point that current begins to flow in the lower section of the main winding. This application of voltage by Q_2 turning on starts the core flux going negative. After a brief transient period, the proper voltages are induced in the base circuits of each transistor, such that Q_1 fully turns off, and Q_2 fully turns on. The cycle is repeated over and over again; this gives rise to the alternating square output waveform desired.

It should be noted that each converter in the two-phase converter shown in Fig. II-3 contains an R-C filter across the two collector terminals and a resistor from the negative dc supply to the common feedback winding lead. The R-C network substantially reduces the emitter-collector voltage transients incurred during operation of the unit into an inductive load (such as a servomotor). Such transients can easily exceed the collector-emitter voltage rating and damage the transistor. The resistor between negative dc and the feedback common aids in initial start-up of the unit.

B. The Phase-Locking Networks

The networks that provide the proper feedback between the two converters in order to insure operation of the units with a 90° phase lag between the outputs is shown in Fig. II-3.

It should be noted that each converter core is identical, and that there are three output windings -- two of 52 turns each and one of 2096 turns. The 52-turn windings may be called W_1 and W_2; the 2096-turn winding serves only as the output winding for each converter.

The windings, W_1, on each core are in additive series with a bridge-rectifier network and reactor L_3. The windings, W_2, on each core are in subtractive series with a second bridge network and reactor L_4; also, L_3 and L_4 are saturable reactors with their volt-time rating equal to one-half that of the main core based on the turns of W_1 or W_2 (equal turns).

Consider the series-adding windings and the bridge network going to the base of Q_1 in unit A. Figure II-4 on the following page illustrates the important voltages.

The reactor L_3 is designed to hold off just $(E_{A1} + E_{B1})\ \tau_1$ volt seconds (τ_1 is one-half the time of a half cycle of output) and to provide a high impedance path to the network as long as the reactor is not saturated. If the phase of either E_A or E_B should happen to drift so that the phase lag were greater than 90°, the volt-time product applied to L_3 would decrease, and nothing would change so far as the L_3 network is concerned. Now, if the phase of either E_A or E_B should drift so that the phase lag were less than 90°, a greater volt-time product would be applied to L_3, and the reactor would saturate. A low impedance path would then be formed, allowing a dc current to flow through the feedback resistor in the base circuit of Q_1. This would, in effect, inject a positive voltage on this base, causing Q_1 to turn off earlier in time than it would have normally. This action would tend to bring the phase relationship between E_A and E_B from less than quadrature to quadrature.

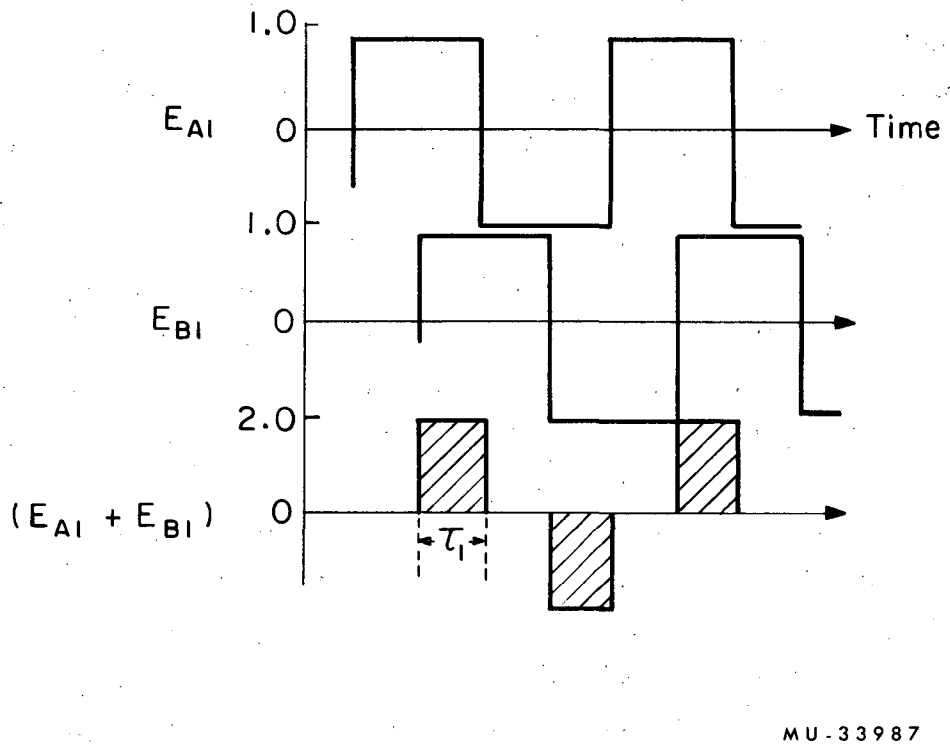

Fig. II-4. Example of main and phase-lock winding voltages.

A similar argument may be applied to the series subtractive network acting on the base circuit of Q_1, unit B. Deviations in phase greater than 90° bring this circuit into play and cause a correction in the firing times of unit B. Phase locking is not affected by inductive or capacitive loading.

C. Specifications on Converter Design

The following specifications were applicable to the design of the two-phase converter for this project:

(1) $5\ V \leq E_{dc} \leq 25\ V$

(2) $40\ V \leq E_A,\ E_B \leq 200\ V$

(3) $12\ cps \leq f \leq 60\ cps$.

The fact that the transistor base should have on the order of 1-V drive influenced the choice of turns ratio in the converter itself. Equation (II-2) is the basic design relation used in selecting the proper core. Also, a balance between wire size (for current-carrying capacity) and core window area was made. The final choice of component values (depicted in Fig. II-3) is somewhat on the overdesigned side, as the converter will be used for other projects in the future.

The total switching capacity amounted to 1220 W.

Figure II-5a shows an oscillogram of both E_A and E_B with the converter operating into the motor. At the time the series of oscillograms in Fig. II-5 was taken, the motor was operating at 1215 rpm and developing a torque of 5.46 oz-in.The component efficiencies at this operating point (heavily loaded) were converter, 82.4%; motor, 10.3%; and overall, 8.5%.

Figure II-5b illustrates the action of the phase-locking circuit in unit A. Here, E_A is shown for reference. An examination of the waveforms shows that the volt-time areas of the phase-locking saturable reactors must not have been exactly balanced, as the converter-output phase lag between E_A and E_B is not exactly 90°.

Figure II-5c shows waveforms of E_A and i_A with the motor as a load. The filter action of the machine inductance should be noted here.

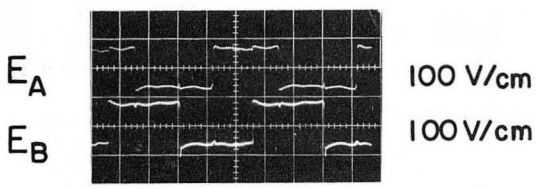

(a)

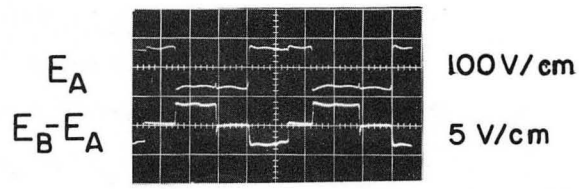

(b)

Horizontal sweep-speed
(All 10 msec/cm)

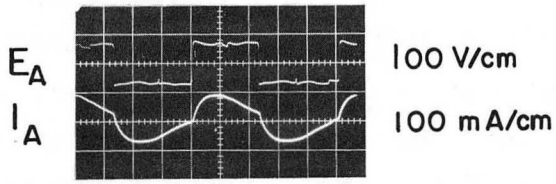

(c)

ZN-4260

Fig. II-5. Converter waveforms.

It should also be noted that the converter output phases maintained balanced levels (rms) throughout the range of input voltage levels.

Figure II-6 is a photograph of the converter during the experimental stages. The four transistors may be seen mounted on heat sinks on the main circuit board. The phase-lock saturable reactors and bridge rectifiers are mounted above the transistors. The two switching cores are at either side of the main board.

The proposed system for obtaining a brushless dc servomotor package and the basic concepts and design of the excitation converter have been set forth in this chapter. The results of the experimental work and critique of these results are discussed in Chapter III.

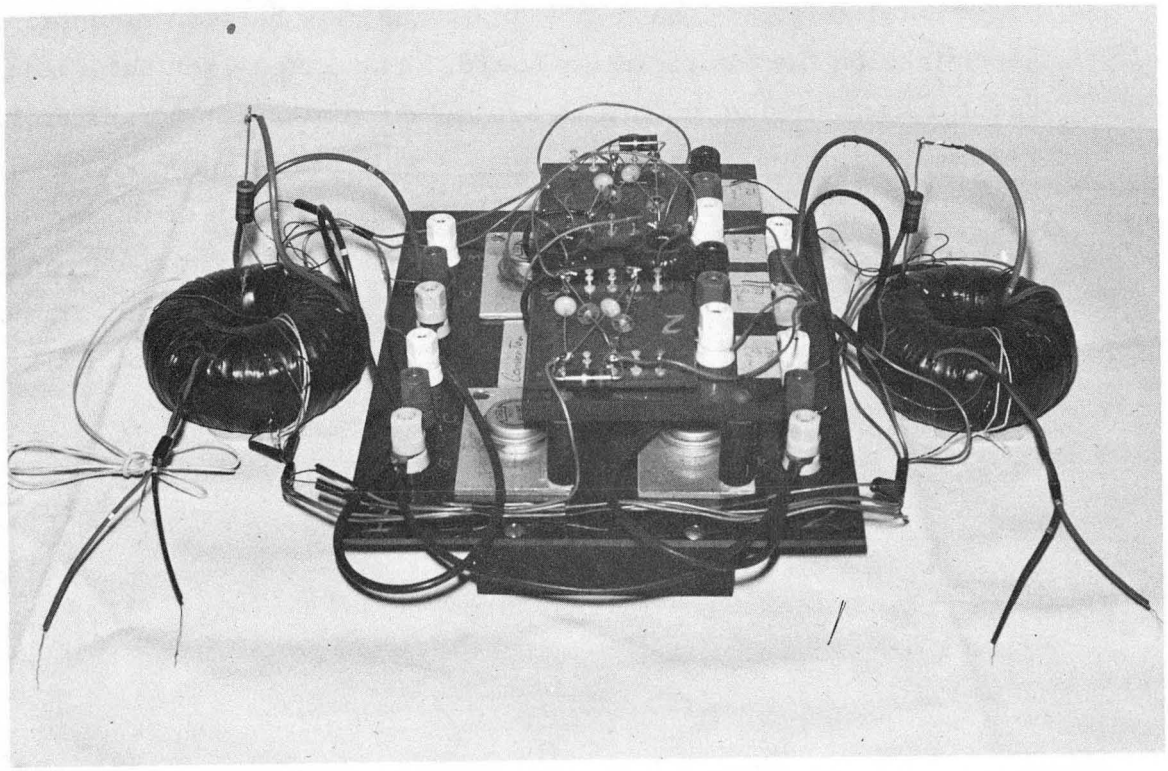

ZN-4261

Fig. II-6. Two-phase transistor converter.

III. EXPERIMENTAL RESULTS AND CONCLUSIONS

In order to evaluate the worth of the brushless dc motor proposed in this thesis, an experimental verification of the predicted steady-state energy conversion characteristics was conducted. Curves depicting the electromagnetic torque developed at various levels of stator current versus rotor shaft speed are shown in Fig. III-1. It can be seen from Fig. III-1 that the torque-speed curves obtained do not follow the predictions made in Chapter II as closely as might be desired. For this reason an attempt is made to understand the major deviations from the predictions. The results of the Appendix--Derivation of the Torque Equation -- are used later in this chapter in order to explain some of the observed results.

A. Instrumentation Methods

The torque-speed curves shown in Fig. III-1 were obtained from a reaction torque dynamometer. A photograph of the dynamometer is shown in Fig. III-2.

The motor was mounted in the cylindrical metal basket (seen in the center of the photograph), and the stator windings were excited by the two-phase converter discussed in Chapter II. Torque readings were taken at various levels of rms phase current with rotor speed held constant. This procedure was repeated for various shaft speeds between 1000 and 3000 rpm. The compilation of torque-speed data is the family of curves seen in Fig. III-1.

Operation of the dynamometer may be described as follows. The motor rotor is coupled to a large variable-speed drive motor mounted on the dynamometer frame. For any one fixed rotor speed, the test motor stator is excited with current of the appropriate frequency. The electromagnetic force developed owing to this excitation tends to accelerate the rotor. As the rotor is fixed at the speed of the large drive motor, the reaction to this acceleration force is a rotational force on the stator. The stator, coupled to the movable basket, rotates about the machine centerline. The basket is attached to the horizontal graduated balance arm and counterweight combination (seen to the left in the photograph).

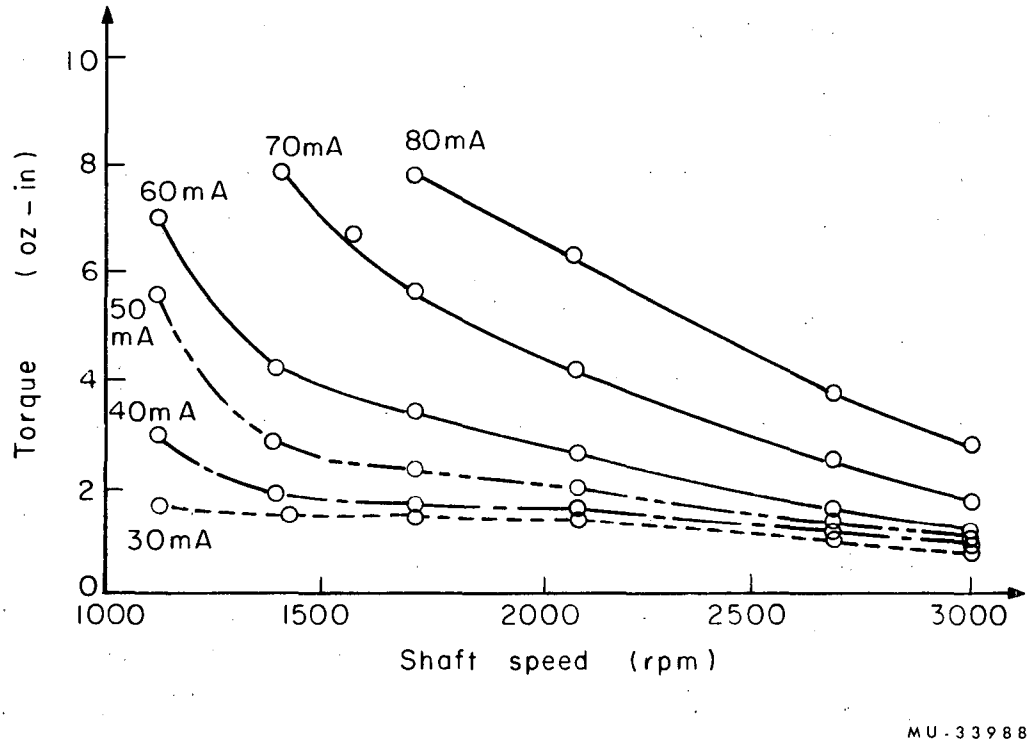

Fig. III-1. Output torque vs shaft speed.

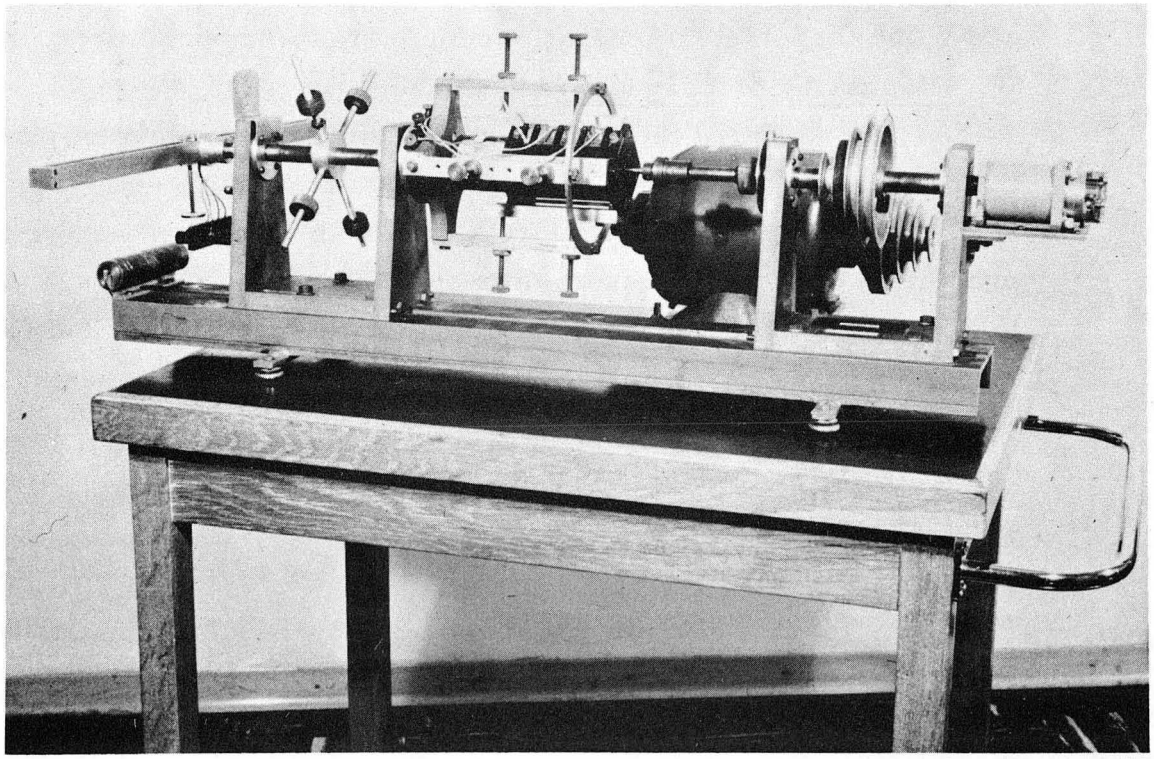

ZN-4262

Fig. III-2. Reaction torque dynamometer.

The reaction torque on the machine stator may then be measured by noting the static balance point on the arm and the value of counterweight needed to produce the balance. The dynamometer is calibrated to 0.1-oz in. torque; however, the accuracy is reduced at high rotational speeds, as vibration affects the balance arm position.

Rotor speed measurements were obtained with a digital counter and pulse tachometer generator coupled to the dynamometer shaft.

B. Discussion of Torque-Speed Curves

The shape of the torque-speed curves for values of phase current between 30 and 50 mA rms (measured by a "true" rms reading instrument) follows --to a reasonable degree -- the general prediction of the brushless motor curves made in Chapter II. For low values of phase current over the entire speed range and for all values of phase current at the higher speeds, the curves tend to become horizontal -- in agreement with Eq. (II-1). A most noticeable departure from the general predictions may be seen as the negative slope characteristic of the curves between 50 and 80 mA.

It is felt that the drop in available motor torque with increasing speed is undesirable from the standpoint of steady-state energy conversion and would reduce the several operating advantages of this motor over other versions of brushless dc motors. For this reason, the equation describing torque production in a synchronous machine having a two-phase stator and permanent magnet rotor was derived. The appendix contains this derivation, along with the necessary assumptions to make the problem tractable, and yields the relationship describing torque production,

$$T = \frac{R}{2} \ell \tau_r B_m C^s I^s \sin \delta, \qquad \text{(III-1)}$$

where R, ℓ, τ_r, and C^s are constants determined by the physical construction of the machine, and the fundamental space harmonic only is considered.

The phase currents were assumed to be "best fit" sinusoids; the peak value of either phase current is I^s. The justification for

using sinusoidal currents in the stator windings rather than some Fourier-series representation of a square wave comes from Fig. II-4c. This is an oscilloscope photograph of the phase current in one stator phase during actual operation. It can be seen that the currents may be approximated by sinusoids with no undue loss in accuracy.

The torque angle, δ, is the angle a rotor reference point makes with a fixed point in the stator-field reference frame and varies with the external load presented to the machine.

The quantity B_m, the maximum flux density in the air gap due to the permanent magnet rotor, is the only term left that could possibly affect the torque production. In order to obtain a constant level of B_m within the air gap during motor operation at various torques and speeds, the magnetic material forming the rotor must not be demagnetized.

The logical explanation for the observed slope of the torque-speed curves shown in Fig. III-1 is that the magnetic material was being demagnetized by increasing amounts as the machine was operated at increasing speeds. It would also be logical to assume that if the rotor magnet were being demagnetized during operation, and the flux density level (B_m) driven down the magnet B-H loop from its normal operating point by large amounts, the internally generated voltages would, over a period of time, be reduced. These voltages (available at either stator phase terminal during open-circuit operation of the machine as a generator) did in fact decrease between the time of initial testing of the machine and the completion of the experimental work. A graph of the internal voltage generated vs speed for the two times noted above is shown in Fig. III-3.

It is felt that a higher-quality magnetic material should be used in the rotor of any future machine based upon the principles discussed in this thesis. The machine selected for experimental verification of the concept for burshless operation described was of World War II vintage; its basic function was a tachometer generator. For these reasons it is felt that the quality of the magnetic material was far from that obtainable from manufacturers today.

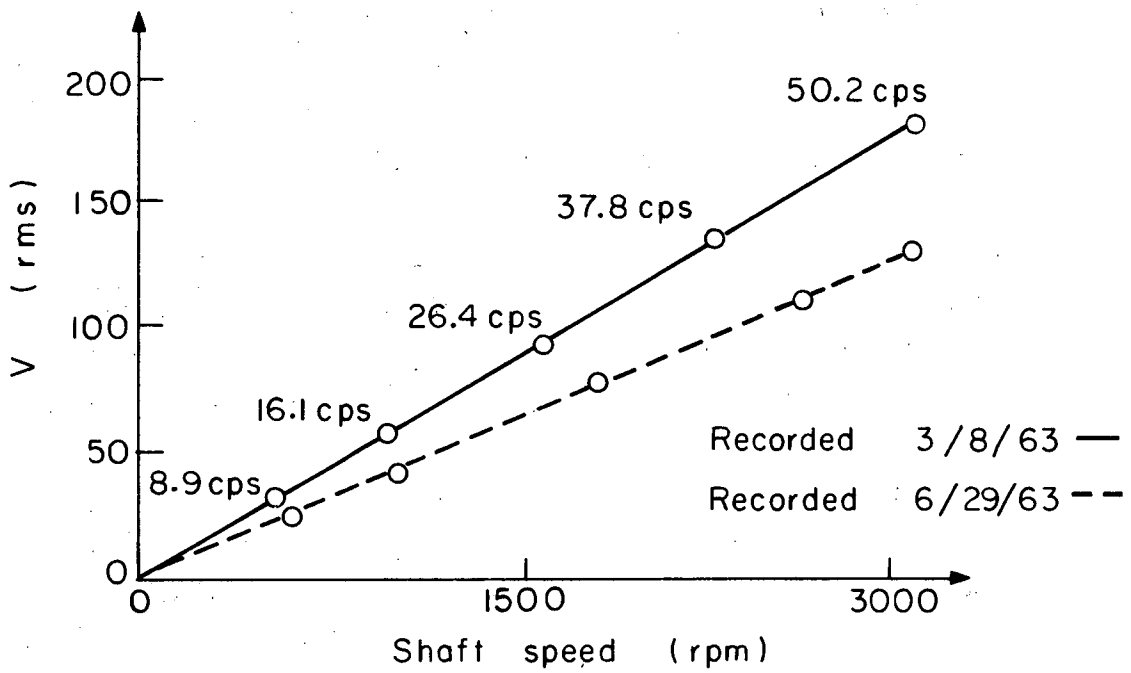

MU-33989

Fig. III-3. Generated open-circuit voltage vs shaft speed (experimental motor).

C. Recommendations for Future Work

As in all conceptual projects similar to the work performed for this thesis, recommendations for future work are appropriate. These should include:

1. Selection of magnetic material of higher quality for the rotor.
2. The incorporation of more than one rotor repeatable section (two poles) for lower-speed operation with the frequency range specified for the converter.
3. The addition of a suitable number of squirrel-cage rotor bars in order to furnish starting torque.
4. Investigation of the dynamic characteristics of the machine for applications in servosystems.
5. The computer analysis of machine operation on a theoretical basis, which includes the effects of space harmonics in the air gap. The correlation of theoretical energy conversion to experimental could then be made on firmer ground.

Not only should the above noted points be considered when additional effort is given to the concept of brushless dc machines, but new ideas for removal of brushes and retaining dc motor characteristics should be aired.

A machine that closely resembles the two-phase motor considered in this thesis, but which operates on discrete pulses of current, is the stepping motor. This machine also has a permanent magnet rotor but has many more repeatable sections over the rotor surface.

It is conceivable that a logical scheme for the generation of the discrete pulses needed to operate a motor of this type could be synthesized. Figure III-4 shows a block diagram of a digital method for obtaining brushless dc motor operation. The power modulator could consist of four switching transistors, one for each motor stator winding. The control pulses to the transistors--pulses that tell the transistors when to fire--are generated in the box labeled "logic elements." These elements could be composed of standard

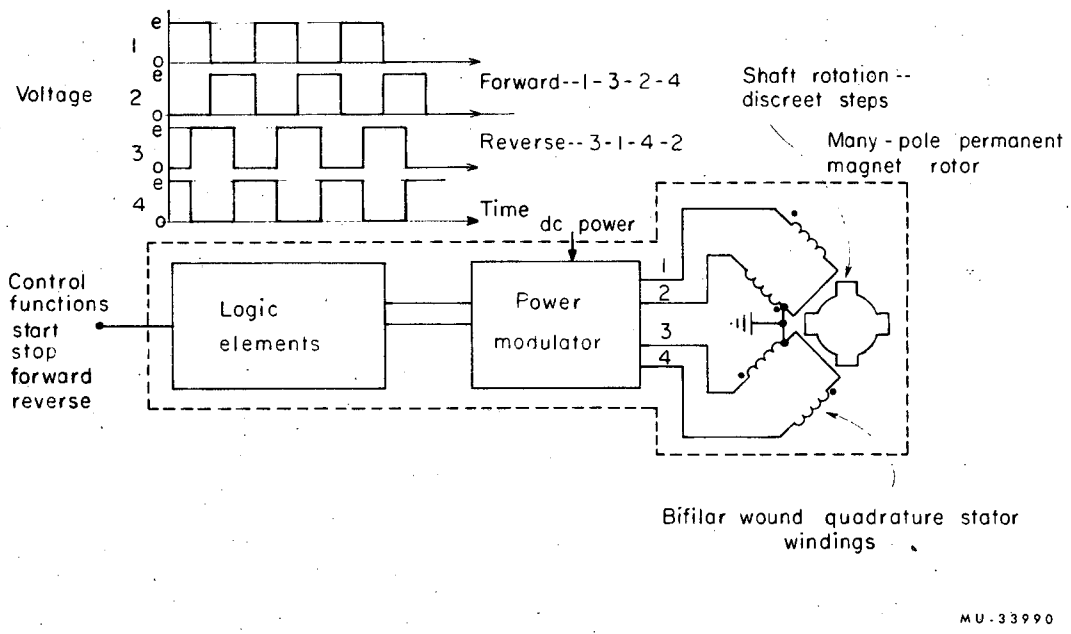

Fig. III-4. A digital scheme for obtaining a brushless dc servomotor package.

pulse gates, inverters, and flip-flops arranged in such a manner as to generate properly timed control pulses. The voltage time plot in Fig. III-4 shows the sequence of application of current pulses to the motor.

A stepping motor with digitally controlled elements operating from a dc power source could be used to great advantage as an extremely accurate positional control servo, and the motor contains no brushes.

D. Conclusions

A new concept for the operation of a dc motor package minus the troublesome brush and bar commutator common to direct-current machinery was examined in this thesis. A previously developed static dc to ac converter that provided two-phase square wave ac was adapted for use as the exciter of the experimental motor. It was found that the actual energy conversion characteristics of the brushless motor deviated from the expected characteristics in several ways. The most adverse deviation was examined with the aid of the derived torque equation applicable to the motor in question. Recommendations for further work on the proposed concept were put forth, along with another scheme for obtaining brushless operation.

This thesis, in essence, has shown that commutators are not really necessary when a rotating energy converter operates from a direct-current source.

It is apparent that there are many ways in which the brushes of a dc motor may be removed. The applications for one particular design of brushless motor may be limited; however, the main point of this work is that it is surely not necessary for the designer to be limited to off-the-shelf machinery when the job calls for rotating machinery.

In the example cited in Chapter I -- dc servomotors in spacecraft -- the main power source could well be direct current. The environment calls for servosystems in which the transducer (error signals to motion) incorporates no brushes. The obvious answer is

the brushless servo; the actual design would depend on the specific requirements of the system.

Judging from the available brushless machines on the open market today, there are indeed applications that justify the need. It will be interesting to follow the market trends and successful applications of these various schemes.

ACKNOWLEDGMENTS

The author wishes to express his appreciation to Professor Robert M. Saunders of the Electrical Engineering Department at the University of California, Berkeley, for the guidance and stimulation he provided during the course of work on this thesis project.

This work was done under the auspices of the United States Atomic Energy Commission.

APPENDIX.

DEVELOPMENT OF THE TORQUE EQUATION FOR A TWO-PHASE SYNCHRONOUS MACHINE WITH A PERMANENT MAGNET ROTOR

A. Derivation of the Torque Equation

A derivation of the equation describing torque production within the machine, during steady-state operation, would show exactly what would produce a variation from the expected torque characteristics as well as predict the shape of the energy conversion curves. The torque equation would contain the actual machine parameters as constants and could be readily applied to the brushless dc machine investigated in this thesis.

The following treatment is based on the work of Saunders[20] and others and is adapted to suit the machine configuration specified in Chapter II of this thesis.

The basic philosophy of Saunders' method of analysis of electromechanical energy conversion systems as applied to double cylindrical structures is the following: By the judicious use of Maxwell's equations in the air gap of a double cylindrical structure, and by the use of a mathematical current sheet set up by current flow in conductors on each or either surface (stator or rotor), the magnetic vector potential within the air gap may be determined. Energy methods then reduce the air-gap energy relationship to an expression relating torque production to the various physical machine parameters and to the excitation currents.

B. Reference Frames

Of prime importance in the following analysis is the transformation of machine cylindrical coordinates to rectangular coordinates (see Fig. A-1).

It can be shown that angular displacement, θ, about the air-gap annulus may be related to linear displacement, x, along the transformed air gap times a constant.[20] Thus

$$\theta \approx a\,x. \tag{A-1}$$

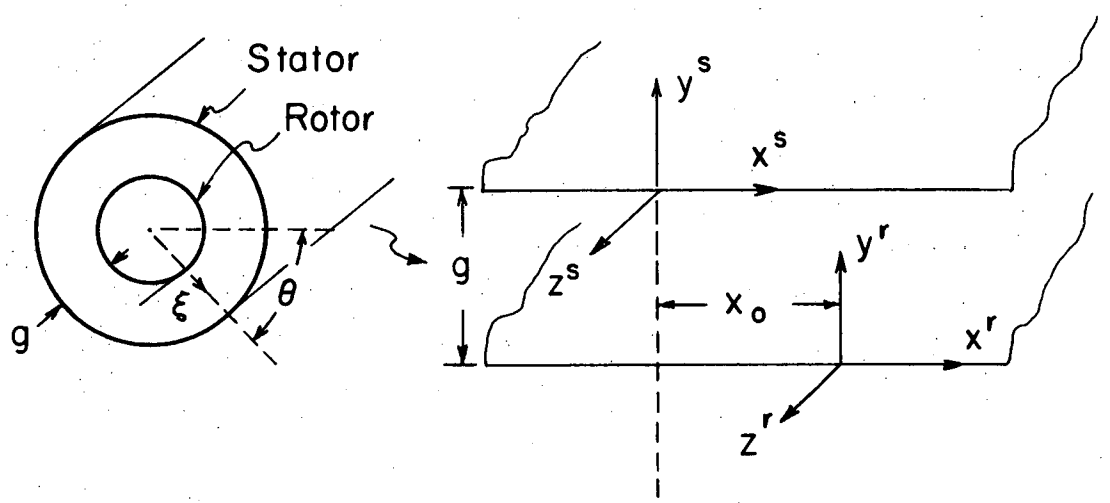

MU-33991

Fig. A-1. Transformation of coordinate axis.

The constant α is related to the length of the repeatable section. The radial distance through the air gap is related to the air-gap coordinate, ξ. Hence,

$$y = \xi, \tag{A-2}$$

where $\xi_{max} = g$, the air-gap distance. Axial distances remain unchanged.

The above transformations are justified provided the rotor diameter is large compared with the air-gap dimension g. In the case of the experimental motor, the rotor diameter was 1.500 in. and the air-gap dimension was 0.0313 in. The stator reference frame, x^s, y^s, z^s, is fixed to the stator surface and is, in fact, the frame of an observer looking at the system. The rotor reference frame, x^r, y^r, z^r, is fixed to the rotor surface and allowed to rotate or move with the rotor. The displacement x_0 then continually increases as the machine is allowed to operate.

It is evident that

$$x_1^s = x_1^r + x_0 \ . \tag{A-3}$$

That is, any point x_1^r can be given a coordinate in the stator reference frame x_1^s by adding x_0 to x_1^r at any instant.

It should be noted that with the foregoing definitions a point x_1^r does not move relative to the rotor reference frame as the rotor moves.

These definitions will be used later in the analysis.

C. Electric-Force Formulation from Energy Consideration

The generalized equation of motion for any electromechanical system can be written as[25]

$$\frac{d}{dt}\left(\frac{\partial \mathcal{L}}{\partial \dot{q}}\right) - \frac{\partial \mathcal{L}}{\partial q} = F_{ext}. \tag{A-4}$$

By setting the generalized velocity, $\dot{q}$, equal to $\dot{x}_0$, the generalized displacement, q, equal to x_0, and the Lagrangian function, $\mathcal{L}$, equal to W_g (the stored energy in the air gap of a machine), we have the mechanical equation of motion of the device,

$$\frac{d}{dt}\left(\frac{\partial W_g}{\partial \dot{x}_0}\right) - \frac{\partial W_g}{\partial x_0} = F_{ext}. \tag{A-5}$$

It will be seen that $W_g \neq f(\dot{x}_0)$; therefore, the equation reduces to

$$-\frac{\partial W_g}{\partial x_0} = F_{ext}, \tag{A-6}$$

or the negative force of electric origin equals the forces of external origin acting on the machine.

Now the term for air-gap stored energy may be expressed as

$$W_g = \int_V \left(\int \vec{H} \cdot d\vec{B}\right) dV = \frac{1}{2\mu_0} \int_V \left(B_x^2 + B_y^2 + B_z^2\right) dV. \tag{A-7}$$

The flux density may be expressed as the curl of the magnetic vector potential. Thus,

$$\vec{B} = \nabla \times \vec{A}, \tag{A-8}$$

or

$$\vec{B} = \begin{vmatrix} \vec{1}_x & \vec{1}_y & \vec{1}_z \\ \frac{\partial}{\partial x} & \frac{\partial}{\partial y} & \frac{\partial}{\partial z} \\ A_x & A_y & A_z \end{vmatrix}. \tag{A-9}$$

D. Magnetic Vector Potentials

If there are j stator phases and k rotor phases, then

$$\vec{A}_{total} = \sum_{j=1}^{m} \vec{A}_j^{\,s} + \sum_{k=1}^{n} \vec{A}_k^{\,r}. \tag{A-10}$$

The solution of Maxwell's equations within the air gap of the machine provides a relationship describing the magnetic vector potential as a function of the machine parameters and the current sheets.[20] The rotor vector potential is not defined as such, as the flux density due to the rotor permanent magnet is available directly (Eq. A-15). The solution for stator magnetic vector potential is

$$\vec{A}_j^s = \sum_{j=1}^{m} i_j^s \left(\vec{1}_z\right) \sum_{\nu=1}^{\infty} \frac{\mu_0 C_{\nu j}^s}{\alpha_\nu} \cos(\alpha_\nu x^s - \phi_{\nu j}^s) \tag{A-11}$$

$$\times (\coth \alpha_\nu g \cosh \alpha_\nu y^s + \sinh \alpha_\nu y^s).$$

The hyperbolic functions in Eq. (A-11) account for the variation of A_j^s in the Y direction.

Equation (A-11) is written so that the order-of-space harmonic, ν, may be as large as deemed necessary. It was felt that a reasonably accurate expression would be obtained by neglecting all space harmonics and considering the fundamental only. The experimental machine was excited with square wave current. Time harmonics due to the excitation may prove more detrimental to operation than space harmonics.

The expression for stator magnetic vector potential reduces to

$$A_j^s = \sum_{j=1}^{m} i_j^s \frac{\mu_0 C_j^s}{\alpha} \cos(\alpha x^s - \phi_j^s)(\coth \alpha g \cosh \alpha y^s + \sinh \alpha y^s), \tag{A-12}$$

and the component is z-directed only.

The term $(\coth \alpha g \cosh \alpha y^s + \sinh \alpha y^s)$ may be approximated by

$$\left(\frac{1}{\alpha g} + \alpha y\right) \text{ implies } \frac{1}{\alpha g} \tag{A-13}$$

if

$$\frac{1}{\alpha g} >> \alpha y.$$

For the experimental motor, $\alpha y_{max} = 0.0416$ and $\frac{1}{\alpha g} = 24.0$.

The magnetic vector potential may then be written as

$$A^s_{j_z} = \sum_{j=1}^{m} i^s_j \frac{\mu_0 C^s_j}{\alpha^2 g} \cos(\alpha x^s - \phi^s_j). \tag{A-14}$$

The flux-density distribution within the air gap due to the rotor permanent magnet may be represented by

$$B^r_y = B_m \sin(\alpha x^r). \tag{A-15}$$

The rotor flux density then varies in a sinusoidal manner within the air gap and is a function of the displacement x^r along the rotor surface.

E. Formulation of the Air-Gap Energy

The stator vector potential has a component only in the z direction; the rotor flux density is y directed. From Eqs. (A-9) and (A-15) we have

$$\vec{B}_x + \vec{B}_y = \vec{1}_x \left(\frac{\partial A^s_z}{\partial y}\right) + \vec{1}_y \left(B^r_y - \frac{\partial A^s_z}{\partial x}\right) \tag{A-16}$$

and

$$\vec{B}_z = 0.$$

The air-gap energy is then

$$W_g = \frac{1}{2\mu_0} \int_V \left[\left(\frac{\partial A^s_z}{\partial y}\right)^2 + \left(B^r_y - \frac{\partial A^s_z}{\partial x}\right)^2\right] dV . \tag{A-17}$$

The integral equation relating the air-gap energy and machine parameters to the generated electrical force is then

$$F_e = \frac{\partial}{\partial x_0} \left\{ \frac{1}{2\mu_0} \int_V \left[\left(\frac{\partial A^s_z}{\partial y}\right)^2 + \left(B^r_y - \frac{\partial A^s_z}{\partial x}\right)\right]\right\}, \tag{A-18}$$

or

$$F_e = \frac{1}{\mu_0} \int_0^{\ell} \int_{-g}^{0} \int_0^{\tau_r} \left[\frac{\partial^2 A_z^s}{\partial x_0 \partial y} \cdot \frac{\partial A_z^s}{\partial y} + \left(\frac{\partial B_y^r}{\partial x_0} - \frac{\partial^2 A_z^s}{\partial x_0 \partial x} \right) \left(B_y^r - \frac{\partial A_z^s}{\partial x} \right) \right] dz^s \, dy^s \, dx^s . \tag{A-19}$$

Using Eqs. (A-14) and (A-15) and carrying out the indicated operations in Eq. (A-19), we have

$$F_e = - \frac{\ell}{\mu_0} \int_{-g}^{0} \int_0^{\tau_r} a B_m \cos a(x^s - x_0) \times B_m \sin a(x^s - x_0) + \frac{\mu_0}{ag} \sum_{j=1}^{m} i_j^s C_j^s \sin(ax^s - \phi_j^s) \, dy^s \, dx^s . \tag{A-20}$$

Note that $x^r = x^s - x_0$ in Eq. (A-3), or

$$F_e = - \frac{\ell g}{\mu_0} \int_0^{\tau_r} a B_m \cos a(x^s - x_0) \times \left(B_m \sin a(x^s - x_0) + \frac{\mu_0}{ag} \sum_{j=1}^{m} i_j^s C_j^s \sin(ax^s - \phi_j^s) \right) dx^s . \tag{A-21}$$

The $\cos a(x^s - x_0) \sin a(x^s - x_0)$ terms integrate to zero, leaving the cosine, sine product with different arguments. Therefore,

$$F_e = - \frac{\ell \tau_r}{2} B_m \sum_{j=1}^{m} i_j^s C_j^s \sin(ax_0 - \phi_j^s). \tag{A-22}$$

For the two-phase machine considered, m equals two; also, the stator field velocity equals the rotor velocity, i.e., synchronous conditions exist.

That is to say, from Eq. (A-3) the following is true:

$$\dot{X}_0 = \dot{X}_s \Rightarrow \alpha\dot{X}_0 = \omega^s \tag{A-23}$$

and

$$X_r = 0, \ \dot{X}_r = 0.$$

Integrating, Eq. (A-23) yields

$$X_0 = \dot{X}_s t + D, \tag{A-24}$$

or

$$\alpha X_0 = \dot{X}_s t \pm \alpha D. \tag{A-25}$$

If Eq. (A-25) were to be transformed back into cylindrical coordinates at this point, $\alpha\dot{X}_s$ would equal ω^s.

The constant of integration αD is either plus or minus, depending upon the operating mode of the machine. For motor operation, as is considered in this thesis, αD is negative. The <u>rotor</u> reference point may be found at any instant by subtracting the displacement αD from the position of a point moving with the stator flux wave.

A more conventional term for the displacement αD (when transformed back to cylindrical coordinates) is

$$\alpha D \Rightarrow \delta, \tag{A-26}$$

the torque angle.

Equation (A-22) may be written

$$F_e = \frac{\ell \tau_r}{2} B_m \sum_{j=1}^{2} i_j^s C_j^s \sin(\alpha\dot{X}_s t - \delta - \phi_j^s). \tag{A-27}$$

Also, 1. $C_1^s = C_2^s = C^s$; stator windings are identical.

$$\left.\begin{array}{l} 2.\ \phi_1^s = 0 \\ 3.\ \phi_2^s = \frac{\pi}{2} \text{ radians} \end{array}\right\}; \text{ stator windings are quadrature-wound.}$$

and

4. $|i_1^s| = |i_2^s| = I^s$; peak value of phase currents is identical.

The phase currents under square wave source excitation were anything but square waves. The low-pass filter action of the machine windings tended to smooth the square current pulses, and the best approximation would be a sine-wave fit for ease of solution.

The illustration below shows the form of phase currents to the machine with a square wave voltage between phase terminals. Figure II-5a is an oscilloscope photograph of motor phase voltage and current during operation.

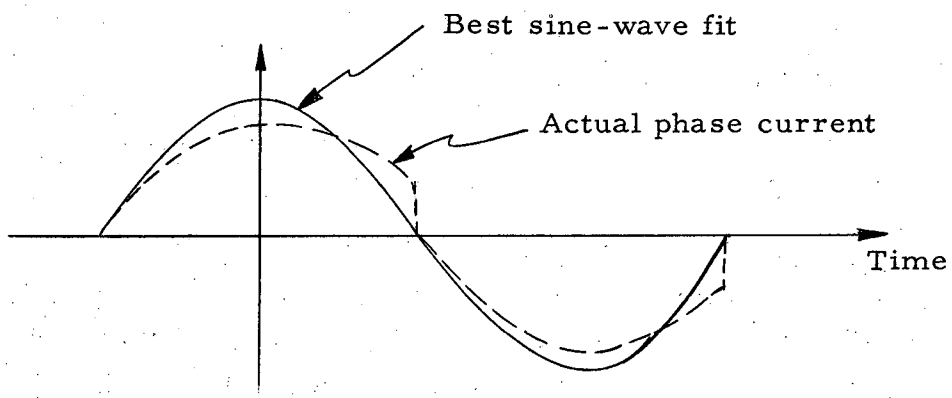

Therefore,

$$i_1^s \approx I^s \cos \omega t = I^s \cos \alpha \dot{X}_s t \qquad \text{(A-28)}$$

and

$$i_2^s \approx I^s \cos(\omega t - \tfrac{\pi}{2}) = I^s \sin \alpha \dot{X}_s t \quad . \qquad \text{(A-29)}$$

The excitation angular frequency transforms to the identical expression for stator flux wave "linear" frequency used in Eq. (A-27). If one considers the relationship between angular synchronous velocity and excitation frequency for the specific motor considered in this thesis, the fact is observed that

$$2 \pi N = \frac{2 \pi f}{(P/2)} \quad , \qquad \text{(A-30)}$$

or, for P = 2

$$\omega^s = \omega^r = 2\pi f = \omega .$$

The force equation is then

$$F_e = -\frac{\ell \tau_r}{2} B_m C^s I^s \left[\cos a\dot{X}_s t \times \sin(a\dot{X}_s t - \delta) - \sin a\dot{X}_s t \cos(a\dot{X}_s t - \delta) \right] . \tag{A-31}$$

Trigonometric manipulation of Eq. (A-31) yields

$$F_e = \frac{\ell \tau_r}{2} B_m C^s I^s \sin \delta . \tag{A-32}$$

If the transformation between cylindrical and rectangular coordinates is linear as assumed, the following is true:

$$T_e = R \frac{1}{2} \ell \tau_r B_m C^s I^s \sin \delta , \tag{A-33}$$

or

$$T_e = K I^s \sin \delta . \tag{A-34}$$

That is, the electrically developed torque depends upon the peak value of phase current (consider a balanced two-phase machine), the sine of the torque angle (δ depends on the load), and a constant composed of factors describing the physical machine dimensions and constants. The torque is constant in time and is not dependent upon the excitation frequency or the rotor angular velocity in any way.

LIST OF SYMBOLS

Symbol	Description	Units
$\vec{A}$	magnetic vector potential	webers/meter
$\vec{B}$	flux density (vector)	webers/meter^2
B_m	maximum rotor flux density	webers/meter^2
C	Fourier coefficient	meters^{-1}
D	integration constant	meters
F_e	forces of electric origin	newton
F_{ext}	forces of external origin	newton
$\vec{H}$	magnetizing force (vector)	amperes/meter
f	frequency	cycles/second
i	instantaneous current	amperes
I	peak value of current	amperes
k	constant	newton-meters/ampere
ℓ	air-gap length in z direction	meters
$\mathcal{L}$	Lagrangian function	newton-meters
m	number of stator phases	----
N	angular velocity	revolutions/second
P	number of machine poles	----
q	generalized displacement	meters
$\dot{q}$	generalized velocity	meters/second
R	radius of rotor	meters
t	time	seconds
v	volume	meters^3
W_g	stored air-gap energy	newton-meters
x	displacement in direction of motion	meters
x_0	displacement between reference frames in direction of motion	meters
y	displacements in radial direction	meters
z	displacements in axial direction	meters
∇	vector differential operator	meters^{-1}

Symbol	Description	Units
α	coefficient = $\frac{2\pi\nu}{\tau_r}$	meters^{-1}
δ	torque angle	radians
ξ	radial air-gap coordinate	meters
θ	angle, phase angle	radians
μ_0	permeability of free space	webers/ampere meter
ν	harmonic order	-----
τ	period of time	seconds
τ_r	length of repeatable Fourier section	meters
ϕ	spacial Fourier phase-angle	radians
ω	angular frequency	radians/second
$\vec{1}$	unit vector	----

BIBLIOGRAPHY

1. E. F. Alexanderson and A. H. Mittag, The Thyratron motor, Electrical Engineering 53, 1517 (1934).
2. Anonymous. Etude d' un Moteur augel des "Thyratron" Servant de Collecteur, Industria Electrique, France, 92, 173 (1933).
3. H. D. Brailsford, Commutatorless dc Motors, U. S. Patents: 2 719 944; 2 753 501; and 2 769 946.
4. H. D. Brailsford, Commutatorless dc Motor Using Transistors, in Proceedings of the National Telemetering Conference (May 1955), p. 53.
5. Brailsford and Company, Type TR Motor (Brochure), (Milton Point, Rye, New York).
6. R. L. Bright, Junction Transistors Used as Switches, Transactions of the AIEE, 34, 111 (1955).
7. D. P. M. Cahill and B. Adkins, The Permanent Magnet Synchronous Motor, in Proceedings of the IEE, London (Dec. 1962), p. 483.
8. S. H. Caldwell, Switching Circuits and Logical Design (John Wiley and Sons, Inc., New York, 1958), Chaps. 1 and 2.
9. W. H. Card, Transistor-Oscillator Induction-Motor Drive, AIEE Communication and Electronics (Sept. 1958), p. 531.
10. J. T. Duane, A Brushless dc Generator for Aircraft Use, Transactions of the AIEE, 77, 365 (1958).
11. D. M. P. Eisenlohr, Transistorized Two-Segment Commutator for a dc Machine, WADC Report 59-683 (Feb. 1960).
12. A. E. Fitzgerald and C. Kingsley, Electric Machinery (McGraw-Hill, New York, 1952), p. 317.
13. A. W. Ford, Brushless Generators for Aircraft, Journal of the Institute of Electrical Engineers, London, 8, 391 (1962).
14. A. Ishizaki, Dynamic Characteristics of a dc Series Servomotor Driven by Thyratrons, Journal of the Institute of Electrical Engineers of Japan, 73, 1269 (1961).

15. E. Kuebler, Der Stromrichtermotor, Elektrotechnische Zeitsehrift, A, Band 79, H. 1, 1.1 (1958), p. 15.

16. Letters to the Editor, Why Not Solid-State Commutators?, Control Engineering (July 1962),p. 14.

17. A. G. Milnes, Phase Locking of Switching Transistor Converters for Polyphase Power Supplies, Transactions of the AIEE, 74, 587 (1955).

18. H. Mogen, Operation of a Saturable-Core Square Wave Oscillator, in Proceedings of National Conference on Aeronautical Electronics, Dayton, Ohio (1956), p. 481.

19. G. H. Royer, A Switching Transistor dc to ac Converter, Transactions of the AIEE, 74, (Part I) 322 (1955).

20. R. M. Saunders, Electromechanical Conversion in Double Cylindrical Structures, IEEE Transactions-Power Apparatus and System (Oct. 1963), p. 631.

21. F. L. Schwartz, Transistorized Four-Segment Commutator for a dc Machine, Massachusetts Institute of Technology WADC Report 59-682 (Feb. 1960).

22. D. A. Steiger, Die Uebertragungsfunktion des Gleichstrommotor mit Thyratrongesteuertem Auker, Regelungstechnik, 5, 47 (1957).

23. P. H. Trickey and T. G. Wilson, dc Machines with Solid State Commutation, AIEE Conference Paper 62-1372 (1962).

24. J. G. Truxal, Ed. Control Engineers' Handbook (McGraw-Hill, New York, 1958), p. 1233.

25. D. C. White and H. H. Woodson, Electromechanical Energy Conversion (John Wiley & Sons, Inc., New York, 1959), p. 205 and 215.

26. D. C. White and H. H. Woodson, Study of Electrical Energy Conversion Systems for Future Aircraft, Massachusetts Institute of Technology WADC Summary Report 59-116 (1959).

27. C. H. Willis, Study of the Thyratron Commutator Motor, General Electric Review, 36, 76 (1933).

This report was prepared as an account of Government sponsored work. Neither the United States, nor the Commission, nor any person acting on behalf of the Commission:

A. Makes any warranty or representation, expressed or implied, with respect to the accuracy, completeness, or usefulness of the information contained in this report, or that the use of any information, apparatus, method, or process disclosed in this report may not infringe privately owned rights; or

B. Assumes any liabilities with respect to the use of, or for damages resulting from the use of any information, apparatus, method, or process disclosed in this report.

As used in the above, "person acting on behalf of the Commission" includes any employee or contractor of the Commission, or employee of such contractor, to the extent that such employee or contractor of the Commission, or employee of such contractor prepares, disseminates, or provides access to, any information pursuant to his employment or contract with the Commission, or his employment with such contractor.